Preprints of the 18th IFAC World Congress
Milano (Italy) August 28 - September 2, 2011

Measurement of Microaccelerations on Board of the LEO Spacecraft

Viktor Fedosov*. Radek Peřestý**

*Aeronautical Research and Test Institute, Beranovych 130 199905, Prague
Czech Republic (e-mail: fedosov@vzlu.cz).
**Aeronautical Research and Test Institute, Beranovych 130 199905, Prague
Czech Republic (e-mail:peresty@vzlu.cz).

Abstract: Aeronautical Research and Test Institute (VZLU) is a joint stock company which serves as Czech national center for research, development and testing in aeronautics and space branches. Since 2002 VZLU has been dealing with development and manufacturing of electrostatic high-sensitive microaccelerometer (MAC) to measure microaccelerations (within the range $\pm$ $2*10^{-4}$ m/s^2) on board of space platforms intended for space science missions (for example, ESA Earth Observation Program or bio/technological research in microgravity conditions). The paper describes principle measurement of the device, instrument performances and application of the accelerometer in recent space research projects. The emphasis will be placed on aspects of accelerometer orbit operation and its functionality verification in orbit.

Keywords: accelerometers, performance characteristics, verification, measurements.

1. INTRODUCTION

Recently, the study of space satellite motion and accurate determination of their orbital elements are giving rise to much interest not only of specialists of astrodynamics in design and predictions of spacecraft orbit but also in some science disciplines such as geophysics, geodesy or navigation. Analysis and correction of Earth's gravitation field, Earth's upper atmosphere parameters and estimation of perturbation effects – this is incomplete list of problems being solved by observation of space satellite motion. As is well known, in Low Earth Orbit, besides gravitational force, a number of perturbing factors influence a spacecraft's trajectory. It is possible to divide these perturbations into two basic groups: gravitational – due to Earth's nonsphericity, other celestial bodies attraction (The Sun, the Moon) and non-gravitational – due to mainly atmosphere drag and direct/indirect solar radiation pressure. In this paper we will try to describe recent achievements of the long lasting effort of Czech academy and industrial research teams on the field of satellite motion perturbation measurement, see L. Sehnal, 1990. Original program goal to study and model perturbing forces have been extended to the development and manufacture of own accelerometer suitable to measure small satellite accelerations. Several technological experiments have been accomplished during last two decades on different satellite platforms.

1.1 Objectives of research program

The objective of *fundamental science* research program is to study non-gravitational accelerations perturbing the satellite motion (Sehnal and Vokrouhlicky, 1995) at low altitudes up to 1000 km. Typical magnitudes of non-gravitational forces acting to a small LEO spacecraft are presented in the Table 1 (for spacecraft with cross sectional area to mass ratio = 0.005 m2/kg, Sehnal, Vokrouhlicky, 1995). For the altitudes below 800 km the atmospheric drag is dominant acceleration (e.g. Bezdek, 2007), higher the direct solar radiation pressure (DSRP) and other radiative forces are greater.

Table 1. Expected values of non/gravitational accelerations in LEO

Acceleration origin	Magnitude [ms^{-2}]
Drag	10^{-4} -10^{-9}
DSRP	~$3x10^{-8}$
Albedo	10^{-8} - 10^{-9}
IR radiation	~$4x10^{-9}$

All these effect have common feature – slow magnitude change with time and position in orbit. For radiative effects the illumination is precondition for acceleration detection. The solar activity has direct impact to the atmosphere drag. Despite of its possible rapid fluctuations the thermosphere response is rather slower. These considerations lead to design performances of accelerometer (as objective of *instrument development* program) for intended purpose, see Table 2.

Table 2. Accelerometer parameters

Accelerometer parameter	Magnitude	SI Unit
Linear range	$\pm$ $2x10^{-4}$	ms^{-2}
Angular range	$\pm$ $9x10^{-3}$	$rads^{-2}$
Linear Resolution	$\pm$ $2x10^{-10}$	ms^{-2}
Angular Resolution	$\pm$ $1.1x10^{-9}$	$rads^{-2}$

2. ACCELEROMETER MAC

2.1 Measurement principle

The instrument consists of one block internally compartmental to the two parts: sensor part and electronic part. Both sections are interconnected by the rigid PCB bus, which carries also external communication and testing connectors. General view of the instrument last model MAC-04 is presented in the Figure 1. On the left side of the figure is electronics part. Sensor surrounded by position detectors is the right side.

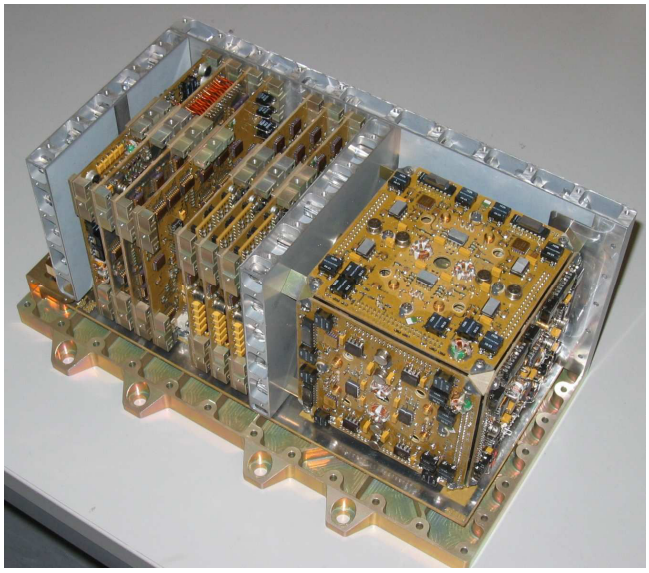

Fig. 1. General view of the accelerometer design (two side plates and cover are dismounted)

The microaccelerometer's sensor is composed of a cubic proof mass free flowing in the cubic cavity. The centre of the sensor should be placed in the spacecraft's centre of gravity. Proof mass is separated from external influences by satellite structure and microaccelerometer construction. Free motion of the proof mass is realized by virtue of only gravitational law. The cavity is rigidly connected to the satellite body. Gravitational and also all other perturbing forces acting on a satellite produce its acceleration and it is the same as the cavity one. The difference between the acceleration of the cavity and the acceleration of the proof mass is the sum of all accelerations produced by non-gravitational forces acting on a satellite. A precise measurement of the proof mass position enables to properly detect its small relative displacements with respect to the satellite-fixed cavity. Applying a known electrostatic force, we can compensate and measure the action of non-gravitational forces. This proof mass position control is performed by feedback servo control electronics. A block scheme of the described proof mass position control system for one axis (for an example, assume that linear channel of measurement) is shown in Figure 2. The constants A1, A2 and A3 represent the shape and geometry of the electrodes and their distance to the proof mass. In this case, we can express acceleration of the proof –mass as function of the regulator voltage U_R and sensitivity of proof mass position detector A3:

$$\Gamma_{pm} = A_1 \cdot U_0^2 (A_2 \cdot x - \frac{U_R}{U_0})$$
$$U_R = A_3 \cdot H_R(p) \cdot x \qquad (1)$$
$$x = \iint (\Gamma - \Gamma_{pm})$$

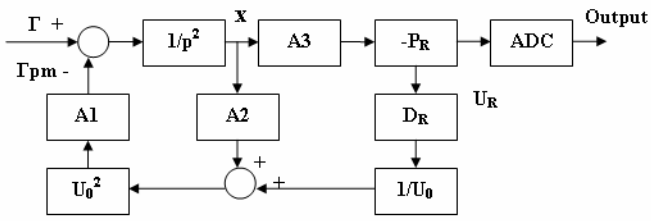

Fig. 2. Block diagram of proof mass position control system

Where:

Γ - input acceleration
Γ_{pm} - proof mass compensative acceleration
U_R - regulator compensative voltage
U_0 - polarization voltage
H_R - regulator transfer function (applied PD regulator consists of **P_R** – proportional action and **D_R** – derivative component)
x - linear shift of the proof - mass
ADC -Analog-to-Digital Converter

Figures 3 and 3a demonstrate response of proof – mass position control system on step of acceleration for linear and angular measurement channels respectively. Figure 4 presents amplitude-frequency characteristic of the instrument at output points of: P Regulator (green curve), D regulator (blue curve) and Anti -aliasing Filter (before ADC, red curve).

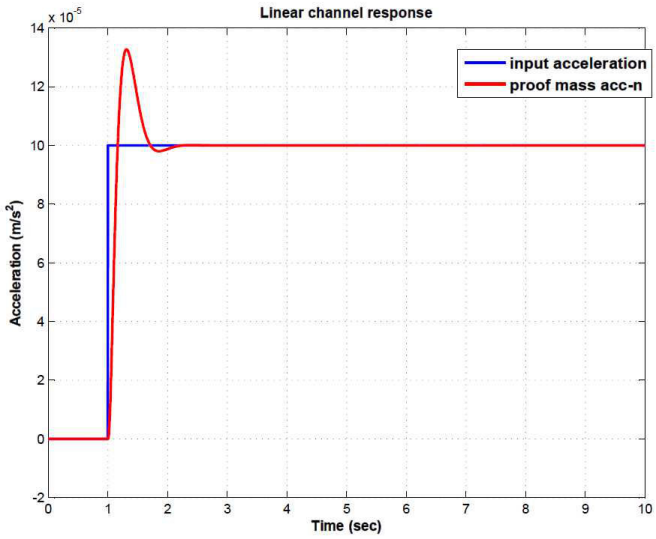

Fig. 3. Linear channel response on acceleration step = 1e-4 m/s2

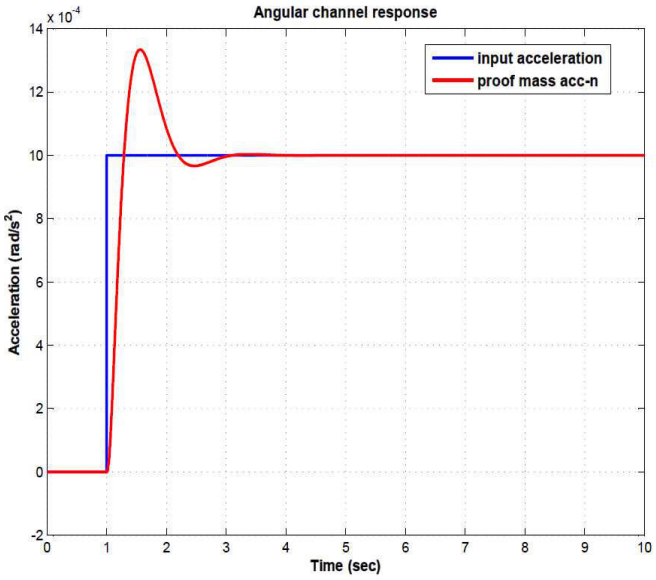

Fig 3a. Angular channel response on acceleration step = 1e-3 rad/s2

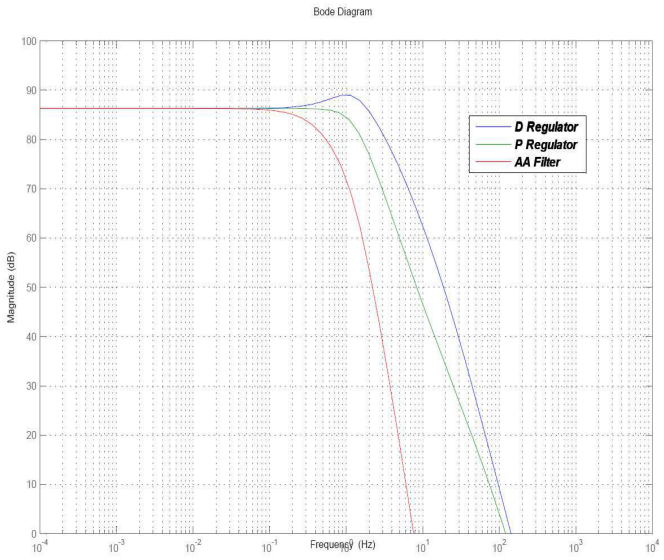

Fig 4 Bode diagrams of PD regulator and ADC components

Amplitude characteristics are flat in the frequency range from 10^{-4} to 10^{-1} Hz (the instrument is efficient for measurement of quasistatic accelerations measurement).

Figure 5 demonstrates simulation of instrument measurements of sinusoidal signal with amplitude = $1*10^{-4}$ ms^{-2} and frequency = 0.01 Hz. Results of the simulation reflect time delay of measured signal (caused by transfer process of input acceleration from sensor to ADC output registers) in relation to input acceleration.

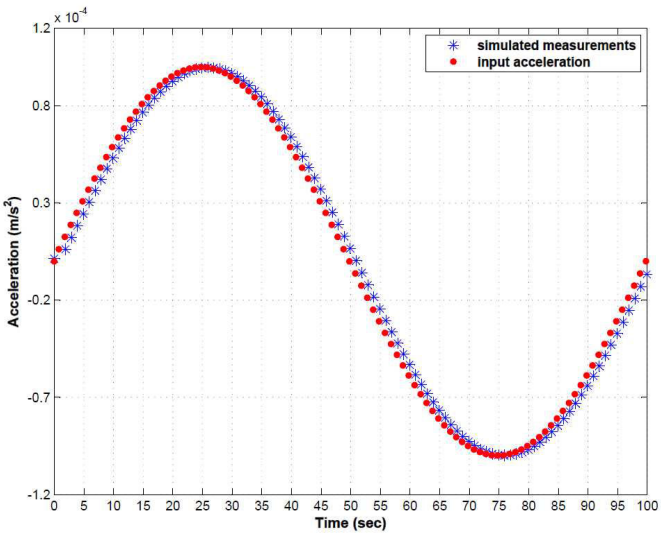

Fig. 5.Simulation of measurement sinusoidal signal (measurement time delay is equal to 1, 2 sec).

2.3 Instrument calibration and characterization

The precise direct on ground characterization and calibration of the instrument is practically not possible for proposed acceleration measurement principle. The main problem is in the generation of tiny force with needed precision and stability in the Earth gravity conditions.

From the above mentioned reasons we apply approach consisting of some steps on two phases of calibration and characterization process.

The first phase of instrument calibration and characterization activity is "On Ground Calibration and Characterization". This phase includes following stages according to the instrument design and manufacturing process:

- **The first** we have to determine theoretical values of characterization parameters of sensor mechanical and electronics during design. The analytical description of the instrument properties and behavior typically represented by the numerical performance model is the result of this step. Preliminary uncertainty estimation is performed by analysis.

- **The second** stage includes as accurately as possible measurement of manufactured characterization parameters for each of device deliverable items. These measurements are performed on the accelerometer manufactured hardware on "low" level of subassembly component. The Instrument Sensitivity is determined. Each parameter is represented by its value and by measurement uncertainty. Then overall accelerometer output

uncertainty from the first step is improved by analysis.

The difference between these two steps is in fact, that in the second stage the direct measurement on manufactured hardware is used for characterization parameters determination and uncertainty analysis, while in the first step is used just theoretical computation and uncertainty estimation. Generally, these steps of characterization are performed during instrument design and manufacturing phase.

- **The next, third** stage is determination of random and systematic component of overall ACC instrument output value uncertainty. The noise frequency characteristics, bias and temperature dependencies of accelerometer output signal are determined. These tasks are performed by the instrument laboratory testing with open control feedback (board level characterization). This stage of characterization runs within the frame of instrument assembling process before start of device verification.

- **Fourth** stage of On Ground characterization is realized during instrument verification process (qualification or acceptance testing) on full assembled instrument level.

Two main different types of tests are needed for finalize On Ground phase of Calibration and Characterization process:

1. Thermal vacuum tests are is intended to produce data sufficient to determine all calibration parameters for linear and angular acceleration measurement channels. There are coefficients expressing temperature dependency of offsets and sensitivities of instrument linear and angular measurement channels. Additionally these tests also produce as a byproduct data sufficient to determine calibration parameters of housekeeping data (in particular linear and angular positions of proof mass and temperatures on position detectors) independently of the board level tests. The thermal vacuum tests are performed at various constant temperatures in the range of -20 °C to +60 °C and under conditions of high vacuum of 10^{-4} Pa. In this step

2. Alignment Tests to determine characterization parameters pertaining transformations of coordinate systems. These tests are performed at laboratory temperature and normal ambient air pressure and humidity and should be done at the end of the testing campaign before instrument integration with a spacecraft.

"In Orbit Calibration" phase is intended for definition of scale factor and bias values including their uncertainty using real measurements of satellite accelerations. Measurements are compared to the etalon acceleration data computed by POD (Precise Orbit Determination) from GPS measurements and satellite attitude data. In orbit calibration process needs discussion exceeding frames of this paper. Detailed description of the calibration method based on POD and modelling the Earth gravitational field are provided by Buinsma et al, 2004 or Bezdek, 2009.

3. MICROACCELEROMETER APPLICATION IN SPACE

During last two decades the accelerometer MAC has been placed on board of several platforms to verify either used technology or to provide science outputs. Obtained results are of different quality. First two experiments (Resouce and Space Shuttle, e.g. Sehnal at all, 2000) were mainly of in-flight technology verification nature. The MIMOSA project was first small satellite dedicated to thermosphere research. Unfortunately the failure of unlocking in one axis spoiled mission goal. Recently the last modification of the accelerometer has been verified on board of Tatiana-2 satellite and results are discussed in hereinafter. The development of accelerometers for ESA SWARM mission is finalized now and qualification for 4.5 year mission is in progress.

MAC04TS is the last modification of the device designed for measurement of spacecraft residual accelerations. The instrument was developed in the frame of project TEASER (Technological Experiment And Space Environment Resistance) which was financed by Ministry of Industry and Trade of the Czech Republic. This instrument has been placed on board of Russian spacecraft Tatyana/ Univerast – 2, see Fig. 6. This small platform was designed for flight testing of new tri-axial stabilization system with low level of produced microaccelerations. Orbit parameters of the Universat-2 are following: circular sun-synchronous, inclination – 98 degrees and altitude is 820 km. Satellite was launched on September 2009.

Unfortunately, after spacecraft separation from the launcher upper stage the satellite stabilization system did not work correctly (infrared Earth sensor failed). Communication with the spacecraft was interrupted after one month operation of the satellite in orbit.

Thus we have to take into account this real platform situation in combination with existence of displacement of the accelerometer relative to the center of mass of the satellite. The proof mass offset will cause that not only accelerations due to the non-conservative forces but also accelerations due to gravitational forces and angular motion act on the proof mass. Hence, the measurement model we can describe as following:

$$\overline{\Gamma}_k = \overline{g}_g + (\overline{\omega} \times \overline{r}) \times \overline{\omega} + \dot{\overline{\omega}} \times \overline{r} + \overline{\Gamma}_i \qquad (2)$$

Where:

Γk – acceleration of the proof mass (measured acceleration)
$\mathbf{g}_g$ – acceleration due to gravity gradients
ω – angular velocity of the satellite
ω' – angular acceleration of the satellite
r – displacement of the accelerometer from the spacecraft center of mass
Γi – non-gravitational acceleration

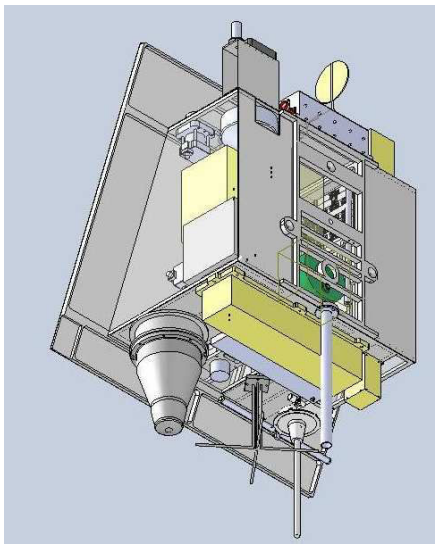

Fig. 6. Russian spacecraft Tatyana/ Universat – 2

As we have possibility (on base of telemetry data) to reconstruct parameters of spacecraft attitude motion (components of satellite angular velocities) than we can estimate the magnitude of microacceleration at instrument position and compare it with measured data. Above mentioned measured acceleration model (see equation (1)) was applied to analysis of data obtained during MAC04TS operation. It has been confirmed that during observation windows the character of the spacecraft angular motion was primary component influencing accelerometer measurements. So, maximum predicted absolute values of non-gravitational accelerations acting along each axis of the satellite reference frame should not be more than 1.93×10^{-8} ms^{-2} (Fig 7), for accelerations rising due to gravitational gradient – 0.64×10^{-9} ms^{-2}. The level of computed values of accelerations rising due to spacecraft rotation was defined as two order bigger ($+3 \times 10^{-6}$ ms^{-2}). The Fig. 8 an Fig. 9 show typical observing window plots of raw data of the accelerometer (green, ms^{-2}) versus angular velocities along X and Y satellite axes (blue, rad/s).

Finally the Fig. 10 demonstrates model describing dependence of measured and smoothed data (blue) on angular velocities (green, along Y, X, Z - high level interventions of stabilization system to stabilize the spacecraft along direction to Earth) and temperature registered at sensor. The time resolution on all figures is one minute.

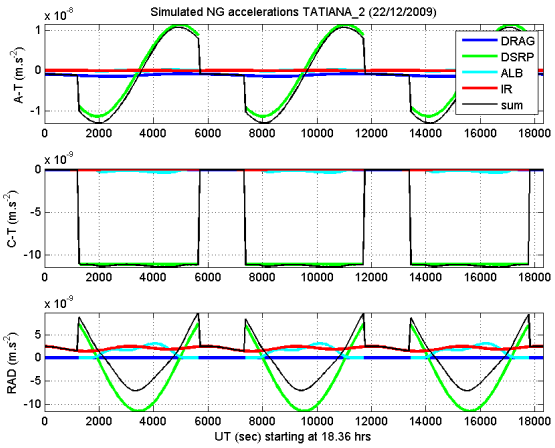

Fig. 7 Exemplification of simulated non –gravitational accelerations for TEASER project conditions/ Simulation has been performed by NUMINSAT (Bezdek et al., 2009)/

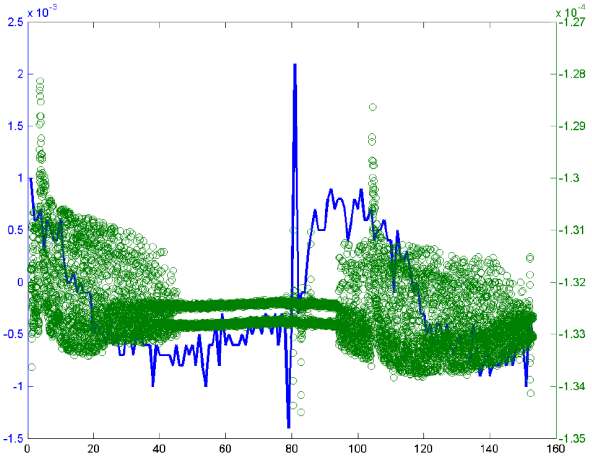

Fig. 8. Spacecraft angular velocity along X axis vs. accelerometer measurements

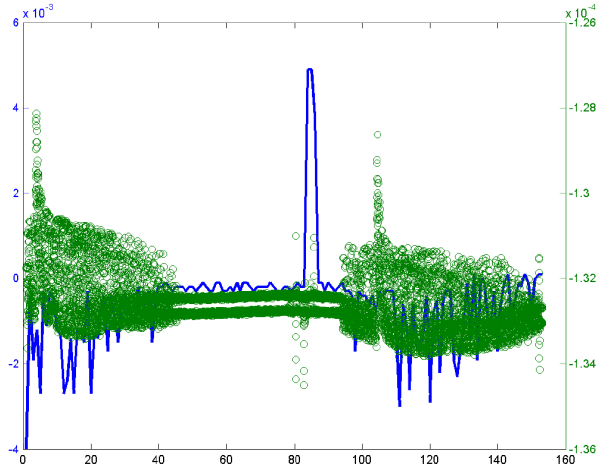

Fig. 9. Spacecraft angular velocity along Y axis vs. accelerometer measurements

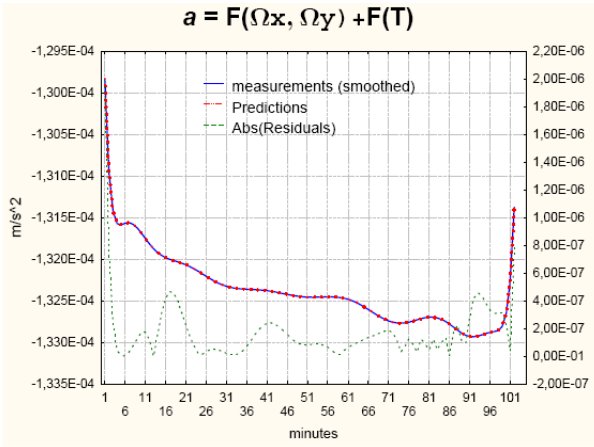

Fig. 10. Accelerometer measurements as function of components of angular velocity and sensor temperature (during one revolution)

4. CONCLUSIONS

The accelerometer developed by Czech industrial teams has partly demonstrated (in flight) its capability to meet required specifications for aimed scientific goals. Recent on ground design verification activities give good chance to meet fully (in combination with in-flight part of calibration) the requirements of the upcoming projects.

REFERENCES

Sehnal, L., 1990. Second order theory of Atmospheric drag Effects, *Space Dynamics*, CNES, Capadues-Editions, Toulouse, France, 1990

Sehnal, L., Vokrouhlický, D., 1995. Model of non-gravitational perturbations for Cesar experiment with Macek accleroemeter. *Adv. Space Res*. Vol. 16, No. 12, pp (12)3–(12)13, 1995

Sehnal, L., Peresty, R., Pospisilova, L., Kohlhase, A., 2000. Dynamical microaccelerometric measurements on board Space Shuttle, *Acta Astronautica* Vol. 47, No.1, pp. 27-34, 2000

Bruinsma, S., Tamagnan, D., Biancale, R., 2004. Atmospheric dencities derived from CHAMP/STAR accelerometer observations. *Planetary and Space Science.* No 52 pp 297 -312.

Bezdek, A., 2007. Lognormal distribution of the observed and modelled neutral thermospheric densities. *Stud. Geophys. Geod*. 51, pp 461–468

Bezdek, A., Klokocnik, J., Kostelecky, J., Floberghagen, R., Gruber, C., 2009 Simulation of free fall and resonances in the GOCE mission. *Journal of Geodynamics*, Vol. 48 No.1, pp 47-53.

Bezdek, A., 2009 Calibration of accelerometers aboard GRACE satellites by comparison with GPS-based non-gravitational acceleration. Poster on ESA's Second Swarm International Science Meeting (available on http://www.congrex.nl/09c24/)